

# TeD-Loc: Text Distillation for Weakly Supervised Object Localization

Shakeeb Murtaza, Soufiane Belharbi, Marco Pedersoli, Eric Granger  
LIVIA, ILLS, Dept. of Systems Engineering, ETS Montreal, Canada  
shakeeb.murtaza.1@ens.etsmt1.ca

## Abstract

Weakly supervised object localization (WSOL) using classification models trained with only image-class labels remains an important challenge in computer vision. Given their reliance on classification objectives, traditional WSOL methods like class activation mapping focus on the most discriminative object parts, often missing the full spatial extent. In contrast, recent WSOL methods based on vision-language models like CLIP require ground truth classes or external classifiers to produce a localization map, limiting their deployment in downstream tasks. Moreover, methods like GenPromp attempt to address these issues but introduce considerable complexity due to their reliance on conditional denoising processes and intricate prompt learning. This paper introduces Text Distillation for Localization (TeD-Loc), an approach that directly distills knowledge from CLIP text embeddings into the model backbone and produces patch-level localization. Multiple instance learning of these image patches allows for accurate localization and classification using one model without requiring external classifiers. Such integration of textual and visual modalities addresses the longstanding challenge of achieving accurate localization and classification concurrently, as WSOL methods in the literature typically converge at different epochs. Extensive experiments<sup>1</sup> show that leveraging text embeddings and localization cues provides a cost-effective WSOL model. TeD-Loc improves Top-1 Loc accuracy over state-of-the-art models by about 5% on both CUB and ILSVRC datasets, while significantly reducing computational complexity compared to GenPromp.

## 1. Introduction

WSOL is a critical yet challenging task in computer vision, aiming to localize objects within images using a model trained using only image-class labels rather

<sup>1</sup>Code is available at [github.com/shakeebmurtaza/TeDLOC](https://github.com/shakeebmurtaza/TeDLOC)

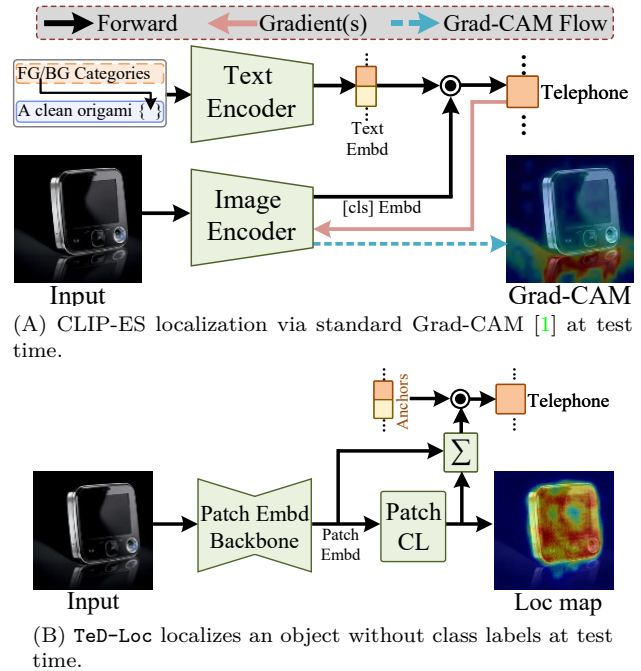


Figure 1. Comparison of our TeD-Loc versus CLIP-ES [1] methods for extracting localization maps from CLIP. (A) CLIP-ES utilizes Grad-CAM to extract localization maps from CLIP, requiring GT class labels during inference. (B) In contrast, our TeD-Loc model distills knowledge from CLIP text embeddings into the visual encoder during training, allowing it to produce both classification scores and localization maps without requiring class labels during inference.

than instance-level annotations. Popular class activation mapping (CAM) method [2] leverage classification models for generating localization maps, however, they inherently focus on the most salient regions of an object and often fail to capture the full spatial extent [3]. This limitation arises because discriminative models are optimized to minimize mutual information between different instances of the same class. Various strategies have been proposed to mitigate this issue, including spa-

tial regularization [4–8], adversarial erasing [9–11], and leveraging pseudo-labeling [3, 8, 12]. However, these approaches are constrained by the local receptive fields of convolutional neural networks (CNNs), which limit their ability to capture global dependencies essential for complete object localization.

Vision transformers (ViTs) [13] have recently shown potential in modeling long-range dependencies through self-attention, thereby mitigating some limitations of CNNs for WSOL. However, they lack the local inductive biases inherent to CNNs, often resulting in weaker local feature representations. Vision-language models, particularly contrastive language-image pre-training (CLIP), have emerged as a promising direction by aligning textual and visual features, which can be leveraged for localization tasks using class-level labels [1]. Yet, the predominant approaches for extracting localization maps from CLIP, such as gradient-based and attention manipulation methods, rely heavily on ground truth (GT) class information. This dependency leads to performance degradation when predicted classes derived from an external model are employed because of feature misalignment and class confusion – exemplified by the frequent conflation by CLIP of similar classes like "airplane" and "aircraft" [14]. Consequently, employing a CLIP model without fine-tuning introduces substantial errors in downstream tasks, prompting the need for strategies that can learn precise localization cues while minimizing reliance on explicit class labels.

Recently, GenPrompt [15] attempted to address these challenges by framing WSOL as a conditional denoising process, leveraging CLIP embeddings to capture discriminative regions. While GenPrompt improves localization by using CLIP embeddings, they still rely on external classifiers or GT class labels during inference, adding to their complexity and limiting their applicability in real-world scenarios. Moreover, despite robust map generation capabilities, a fundamental limitation remains the inability of CLIP-based methods to localize objects within an image without prior class information. This constraint poses a significant challenge for downstream tasks, as they require computing class labels beforehand (Fig. 1A). Given these challenges, we seek to effectively harness vision-language models to learn precise localization cues for WSOL, while mitigating misclassification and reducing reliance on GT labels during inference.

To address these challenges, we propose Text Distillation for Localization (TeD-Loc), which learns to localize by distilling knowledge from CLIP text embeddings because they serve as a powerful link between visual and textual modalities. It learns localization in-

formation by transferring knowledge from text embeddings to the localization module (Fig. 1B). Using contrastive learning within a teacher-student framework, the visual representations of our model are aligned with text embeddings. This alignment is guided by pseudo-labels that can be extracted from any CAM-based method. Learning from text embedding allows TeD-Loc to achieve state-of-the-art performance using one model selected using the best localization performance without requiring separate classifiers trained and selected using the validation set over the classifier’s score. TeD-Loc introduces a new paradigm where classification is achieved through localization, thereby eliminating the need for model selection over the classifier’s score. By training the  $E_V$  to distinguish between foreground (FG) and background (BG) regions based on their similarity to text embeddings, TeD-Loc enables the model to classify and localize objects simultaneously. Furthermore, to address the limitations of CLIP’s frequent conflation of semantically similar classes, we propose a method to orthogonalize text embeddings before distillation. By default, text embeddings in CLIP may not sufficiently discriminate between similar classes because of their proximity in the embedding space. To mitigate this issue, we decompose the embeddings using QR decomposition [16] and utilize the resulting orthogonal basis vectors for alignment.

More specifically, our method employs a transformer-based architecture that decomposes an image into a set of patches, generating upsampled patch embeddings through our model backbone. Each patch embedding is individually classified to estimate its likelihood of representing a FG or BG region. These classification scores are then stitched together to produce a localization map, highlighting regions of interest within the image. The global classification score for the entire image is a weighted average of the patch embeddings, where the weights are derived from the classifier scores. Our approach is inspired by the multiple instance learning (MIL) framework, where each image consists of a “bag” containing multiple “instances” (image patches) with only bag-level labels available during training. Leveraging MIL, object localization and classification are performed simultaneously by assigning higher weights to discriminant patches, without relying on external classifiers or prior class information. This aligns well with the weakly supervised nature of object localization, enabling our model to independently produce accurate localization maps and classification scores.

Our main contributions are summarized as follows.  
**(1)** A novel TeD-Loc method is introduced that dis-

tills knowledge from the CLIP  $E_T$  to guide object localization using pseudo-labels extracted from CLIP. By leveraging the synergy between visual and textual embeddings, TeD-Loc effectively identifies FG regions and suppresses BG noise without resorting to manual prompt engineering or defining BG categories for each dataset.

(2) A new module is proposed to transfer knowledge from text embeddings to pixel levels, ensuring that FG and BG embeddings are separated. By maximizing the similarity between FG patch embeddings and text embeddings, the model aligns visual and textual modalities. Further, we employed a localization module to map these patch embeddings to FG/BG regions producing localization maps.

(3) A classification module is introduced to leverage localization scores to compute the expected embeddings of FG regions. Using a weighted average of patch embeddings, where the weights are derived from the FG localization map, we ensure that FG embeddings align with the correct class embeddings. This eliminates the need for an external classifier and allows our model to classify and localize simultaneously.

(4) To mitigate the tendency of CLIP to conflate semantically similar classes due to proximity in its embedding space, we propose orthogonalizing text embeddings before alignment. This reduces embedding overlap, allowing our model to achieve competitive performance across both localization and classification tasks.

(5) Extensive experiments on the challenging CUB and ILSVRC datasets show that our proposed strategy can outperform state-of-the-art methods in terms of Top-1 Loc performance, yet significantly reduce computational complexity versus GenPromp.

## 2. Related Work

(a) **Weakly supervised object localization.** WSOL is a challenging task that seeks to localize objects using only image-level supervision. The foundational work in WSOL [2] proposes to harvest CAMs from pre-trained CNNs, leveraging global average pooling (GAP) to guide the network’s attention toward specific regions in an image. Despite its impact, CAM and related CNN-based approaches are constrained to highlight discriminative regions, often neglecting complete object extents. This limitation has led to the development of different WSOL methods that can look beyond discriminative regions.

Erasing-based methods aim to mitigate CAM partial activation by selectively obscuring parts of an image to encourage broader localization. HaS [17] and CutMix [7] employ random erasure, which forces the network to explore different object parts beyond dis-

criminative regions. Building on this, adversarial erasing methods like ACoL [9] and ADL [10] use dual classifiers to identify and erase dominant regions, uncovering complementary object regions. Techniques like SPG [8] go further, integrating pixel-wise correlation constraints to maintain context and consistency across object regions.

Other works target the inherent challenge in CNNs to capture only local semantic features due to limited receptive fields. Consequently, newer methods leverage structural cues and integrate BG suppression techniques. SPA [18] enhances structural consistency, while PSOL [19] introduces a two-stage WSOL approach that decouples classification from localization tasks, providing robust pseudo annotations for regression without class constraints. Methods such as BAS [5] reinforce this separation by suppressing BG regions, emphasizing FG areas critical to localization.

To overcome the inherent CAM limitations in capturing long-range dependencies, transformer-based approaches for WSOL are gaining traction. Transformers, known for their self-attention mechanism, enable networks to capture both local and global feature dependencies. Vision Transformer (ViT) [20] and DETR [21] demonstrate the potential of self-attention in vision, and in WSOL, TS-CAM [13] leverages token-patch fusion with semantic maps to improve spatial coherence. By exploiting transformers’ long-range capability, these methods significantly broaden the object localization scope and address the core issues of CNN-based localization methods.

(b) **Contrastive language–image pre-training.** CLIP [22] is a foundational model designed to align visual and language representations, trained on 400 million image-text pairs collected from web data. By learning from paired data, CLIP produces a robust model capable of zero-shot adaptation to diverse tasks by computing similarities between images and textual descriptions. In WSOL, GenPromp leverages CLIP to identify discriminative regions and employs VQGAN for embedding generation within a denoising process to localize objects; however, its computational complexity hinders real-time applicability.

Moreover, CLIP has been widely adapted for weakly supervised semantic segmentation (WSSS), prompting multiple approaches to leverage its capabilities for generating class activation maps (CAMs) without extensive labeled data. For instance, CLIMS [23] utilizes CLIP to enhance the completeness of object regions within CAMs while suppressing BG regions. CLIP-ES [1] employs GradCAM to extract CAMs directly from CLIP, demonstrating that activations can be generated without fine-tuning. SCLIP [24] and NA-

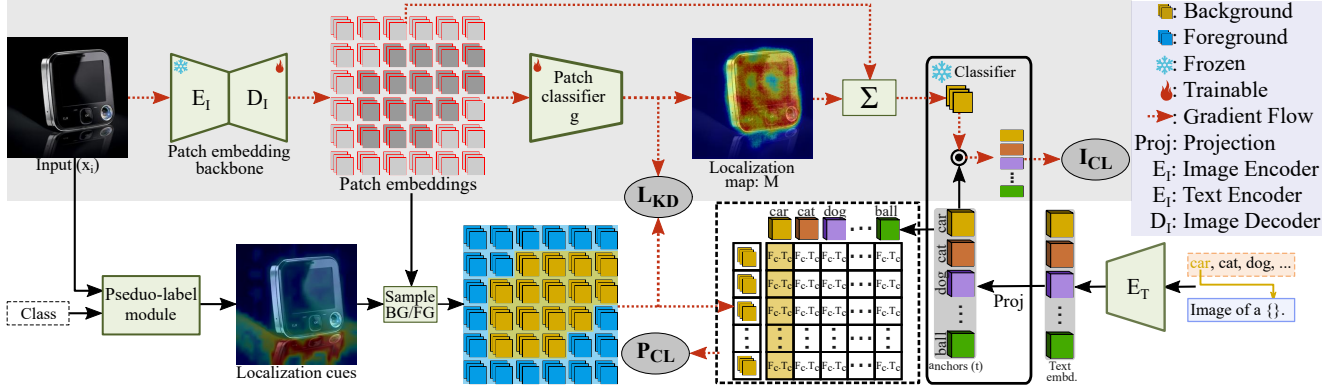


Figure 2. Overview of the **TeD-Loc** method for distilling FG text embeddings into the patch embedding backbone. First, pseudo-labels are extracted to guide the identification of FG and BG patches. By leveraging these FG/BG regions, the model minimizes the similarity of  $E_V$  with the relevant text embedding for FG classes, while maximizing dissimilarity with embeddings of other classes. Through a binary FG/BG classifier, **TeD-Loc** generates localization maps by classifying patches as FG or BG, while generating class probabilities for image classification. This joint task enables the model to produce both accurate localization and classification outputs without explicit bounding box supervision.

CLIP [25] propose modifying the last attention block to produce score maps for each patch embedding, enabling segmentation map generation without requiring a backward pass. Similarly, [26] introduces learnable prompts in CLIP and uses pseudo-labels from SAM [27] to fine-tune for WSSS.

While CLIP-based methods yield competitive maps, these methods rely on hand-crafted textual templates and predefined class representations — such as prompts like “a photo of [CLS].” This requires prior knowledge of the specific class name before producing a localization map of each image. This reliance restricts the model’s adaptability across different computer vision tasks. It also leads to substantial performance degradation when using predicted classes, due to feature misalignment and class confusion. These limitations underscore a critical challenge: the need for WSOL methods that can learn precise localization cues without reliance on explicit class labels or predefined textual templates. To address this challenge, we propose a novel method that distills knowledge from CLIP’s text-image representations to guide the localization network. Additionally, we mitigate the tendency of CLIP to conflate semantically similar classes by orthogonalizing the text embeddings before alignment, reducing semantic overlap and improving discriminability. This enables the model to classify the image by computing the similarity between visual embeddings and class anchors as visual embeddings are pushed toward class-text embeddings.

### 3. The Proposed Method

Let us consider a training set  $\mathbb{D} = \{(x_i, y_i)\}_{i=1}^N$  of  $N$  images, where each image  $x_i \in \mathbb{R}^{H \times W \times 3}$  is associated with an image-level label  $y_i \in \{1, \dots, K\}$ , representing one of  $K$  object classes, with no bounding box (bbox) supervision. WSOL methods seek to train a model for object localization and classification using only image-level labels. In this paper, we leverage text embeddings from a pre-trained vision-language model, specifically CLIP [25].

Our model (see Fig.2) consists of three modules, — a patch embedding backbone network and a compact head for localization and classification tasks. The backbone network is comprised of the (i) *Encoder E*, a ViT (ViT-EVA-L) [28] that decomposes images into patches and produces patch-level embeddings. It is pre-trained for classification and frozen during training. (ii) The *Decoder D* upscales these patch embeddings to a high spatial resolution where the  $p^{\text{th}}$  output patch is denoted as  $z_p$ . The CLIP text encoder is denoted as  $E_t$ . Moreover, we introduce a binary patch classifier  $g(z_p)$  that predicts the FG/BG for each patch. Its response over all the patches forms a localization map  $M$  containing the FG object associated with the image class. This map provides the localization generated by our method. Furthermore, we define the classification scoring function  $f: \mathbb{R}^d \times \mathbb{R}^d \rightarrow \mathbb{R}$ , which is parametrized with *frozen* class weight vectors  $t_k \in \mathbb{R}^d$  for a class  $k$  for  $k \in \{1, \dots, K\}$ . An embedding vector  $v \in \mathbb{R}^d$  is required. It computes its score for a class  $k$  via its dot product with the class anchor  $t_k$ :  $f(v, t_k) = \langle v, t_k \rangle$ . In this work, we consider  $t_k$  as the CLIP text embedding

of the class  $k$ , while  $v$  could be a patch embedding  $z_p$ , or the global image embedding  $h$  of our method.

### 3.1. Key Components

The rest of this subsection introduces two important components of our TeD-Loc method – the generation of pseudo-labels of patches and the pre-processing of text embeddings.

**Patch-level pseudo-label generation.** To train our model we propose to leverage patch-level pseudo-annotation corresponding to FG and BG patches. However, since such annotations are not available in the WSOL setting, we consider an off-the-shelf pre-trained CAM-based classifier. Such models can yield a discriminative map to localize a target class which is adequate during training. Generally, any CAM-based model can be used [29–31] to generate localization cues that can be leveraged for training. During the training of our model, we randomly sample few FG/BG patch locations for each training image at each training step to avoid overfitting. This pseudo-labelling technique has been shown to be effective in guiding learning [3, 32]. In our experiments, we sample the same number of FG/BG locations to maintain a balanced ratio between the two classes.  $\omega$  denotes the set containing the sampled patches for both FG/BG while  $\omega^+$  contains only the selected FG patches.  $y'_p \in \{0, 1\}$  is used as the patch pseudo-label where 0 is BG and 1 is FG. Additional details on this pseudo-labelling process are provided in suppl. materials.

**Text embeddings orthogonalization.** CLIP text embeddings of classes are used to distill localization knowledge as they provide a powerful link between visual and textual representations. However, they can sometimes conflate similar classes due to semantic overlap (e.g., “airplane” and “aircraft”) [14]. This overlap between classes limits the benefit of those embeddings, especially when used in discriminative scenarios. To mitigate this issue, we propose to pre-process the class-text embeddings before using them in our method. We consider a transformation that projects all the text embeddings into a space where the distance between each pair of embeddings is maximum. In this work, we use orthogonal projection, in particular, QR orthogonalization [16] and conserve the basis of the projection. In the rest of this paper, the orthogonalized version of text embeddings for class  $k$  are referred to as  $t_k$ . These new embeddings are kept frozen and play the role of class anchors that are carried with our model allowing us to discard the text encoder. We illustrate the issue of class overlap and the impact of orthogonalization over text embeddings in Fig.3.

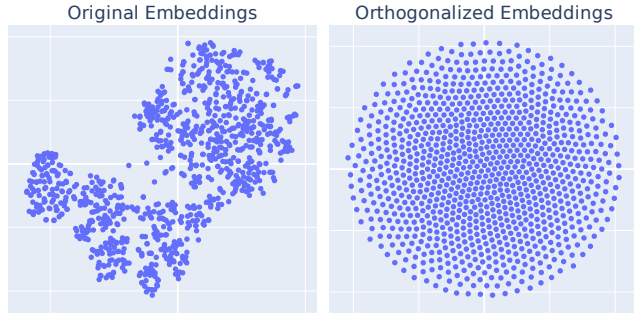


Figure 3. t-SNE visualizations of CLIP text embeddings for ILSVRC [33] classes before and after orthogonalization. **(Left)** Prior to orthogonalization, embeddings of semantically similar classes (e.g., “airplane” and “aircraft”) cluster closely together, leading to potential confusion. **(Right)** After orthogonalization (QR decomposition), the embeddings are more uniformly distributed and orthogonal, reducing overlap.

### 3.2. The TeD-Loc Training Method

**Text embedding distillation to local patches.** Our objective is to distill text-class embeddings into patch embeddings and to discard the text encoder. Since text and global image embeddings in CLIP are not directly tied to patch embeddings, text embeddings cannot directly be used to localize objects. Patch embeddings are not necessarily correlated with text embeddings [34]. In this work, we propose to create a direct link between text embeddings and patch embeddings for semantic localization. To achieve this, we propose to use knowledge distillation where we transfer text embedding of the image class to the patch embeddings allowing us to perform object localization. In particular, a contrastive learning loss [22] is employed to ensure that FG patch embeddings are similar to text embedding of the image class while being dissimilar from embeddings of other classes. To this end, only the FG patches  $z_p$  where  $p \in \omega^+$  are used for this loss. It can be simply defined through a standard cross entropy as follows [22],

$$\mathbf{L}_{\text{KD}} = \sum_{p \in \omega^+} CE(y, f(z_p, t_y)). \quad (1)$$

Equation 1 is computed only on the selected FG patches  $\omega^+$ , as BG patches lack corresponding class embeddings, rendering them unsuitable for this contrastive loss. Since BG is not considered this can lead to poor localization as the BG region is present in most images. To mitigate this issue, we introduce a patch binary FG/BG classifier  $g$  which repels BG patch embeddings from FG text embeddings. It is trained using both FG/BG patches  $z_p$  and their pseudo-labels  $y'_p$  via

standard cross-entropy loss,

$$\mathbf{P}_{\text{CL}} = \sum_{p \in \omega} CE(y'_p, g(\mathbf{z}_p)). \quad (2)$$

Minimizing this loss allows for both FG and BG regions to be present in the image which helps avoid imbalanced localization.

**Global image embeddings from local patch embeddings for classification.** So far, our method can only perform localization. To further allow it to perform image classification, our aligned FG patch embeddings are leveraged to construct global image embedding that describes the object in the image. This creates a reversed link from local patch representations to global image representation allowing to learn to classify the image. This aligns perfectly with our distillation approach from class text embedding to patch embeddings described previously, where we ensure that FG patch embeddings are correlated with the text embedding of the image class. Therefore, we leverage this property to construct a global image embedding  $h$  using all the patch embeddings and the patch classifier  $g$  as follows,

$$h = \sum_p a_p z_p, \text{ where } a_p = g(z_p) / \sum_j g(z_j). \quad (3)$$

Eq.3 performs a weighted average of the embeddings for all the patches by giving more importance to patches that are classified as FG since their  $g(z_p)$  will be closed to 1. In addition, BG patches are discarded since  $g(z_p)$  close to 0. This effectively performs a differentiable selection of FG patches allowing for training with gradient-based methods. Most importantly, the final aggregated embedding  $h$  is expected to resemble the text embedding of the image class  $t_k$ . To further ensure this, this embedding is trained to be as close as possible to  $t_k$  using standard cross entropy as follows,

$$\mathbf{I}_{\text{CL}} = CE(y, f(h, t_y)). \quad (4)$$

**Overall training loss.** Our overall training loss contains the three terms discussed previously: knowledge-distillation loss ( $\mathbf{L}_{\text{KD}}$ ), patch classifier loss ( $\mathbf{P}_{\text{CL}}$ ) and global image classification loss ( $\mathbf{I}_{\text{CL}}$ ) as follows,

$$\mathbf{L} = \lambda_1 \mathbf{L}_{\text{KD}} + \lambda_2 \mathbf{P}_{\text{CL}} + \lambda_3 \mathbf{I}_{\text{CL}}, \quad (5)$$

where  $\lambda_1$ ,  $\lambda_2$  and  $\lambda_3$  are weighting factors that balance the contribution of each term. Stochastic Gradient Descent (SGD) is used for optimizing the parameters of our model which consist of the parameters of the decoder  $D_I$  and patch classifier  $g$ . By jointly optimizing these loss functions, our model learns to produce discriminative and well-aligned visual representations, enabling simultaneous classification and localization.

## 4. Results and Discussion

### 4.1. Experimental Methodology

**Dataset.** Two common challenging datasets were used for our WSOL experiments: (i) Caltech-UCSD birds-200-2011 (CUB) [35] consists of 11,788 images spanning 200 bird species. The dataset is partitioned into 5,994 training images and 5,794 testing images. For validation, an independent set of 1,000 images (five per class) collected by [29] is utilized. (ii) ImageNet large-scale visual recognition challenge (ILSVRC) [33] includes approximately 1.2 million training images and 10,000 validation images across 1,000 classes. We use the original validation split as our test set due to its sufficient size for robust evaluation. For validation purposes, ILSVRC-V2, collected by [36] and annotated by [29], is employed to mitigate biases toward the test set. For a fair comparison, we strictly adhere to the commonly used WSOL protocol proposed in [29] for both datasets.

**Evaluation measures.** Following earlier work by Choe et al. [29], we employ three localization measures alongside one classification measure to evaluate the proposed method. The localization measures are as follows: (1) **MaxBoxAcc** (referred to in previous work as **CorLoc** [37] or **GT-Known** [17]), which quantifies the proportion of images for which the predicted bbox achieves an Intersection over Union (IoU) threshold of  $\sigma = 50\%$  with the ground-truth bbox, independent of classification accuracy (**CL**); (2) **Top-1 Loc**, measuring the proportion of images where the model’s top predicted class is correct and the bbox IoU with ground truth exceeds  $\sigma = 50\%$ ; and (3) **Top-5 Loc**, defined as the proportion of images for which the true class label is within the model’s top-five predictions and the bbox meets an IoU of  $\sigma = 50\%$ .

**Implementation details.** We closely followed the experimental setup of Choe et al. [29], dataset splits, evaluation of localization maps across multiple thresholds, and training epochs—specifically, 50 epochs for the CUB dataset and 10 epochs for ILSVRC. Furthermore, our model is trained with a batch size of 32 and 16 for ILSVRC and CUB, respectively. In Eq.5, the hyperparameters  $\lambda_1$ ,  $\lambda_2$  and  $\lambda_3$  used in the total training loss (Eq.5) terms that are optimized over the values (0, 1]. Optimization of our model was performed using SGD, with a learning rate from 1e-6 up to 0.01. We also fine-tuned the weight decay and momentum parameters. Generated localization maps were evaluated at a resolution of  $256 \times 256$  pixels.

**Baseline methods.** To extensively evaluate the performance of **TeD-Loc**, we compare against several recent state-of-the-art WSOL methods, includ-

ing TS-CAM [13], SCM [38], LCTR [39], C<sup>2</sup>AM [40], PSOL [19], DiPS [32], CATR [41], DA-WSOL [42], BAS [5], and GenPrompt [15]. Additionally, CLIP-ES [1], which utilizes Grad-CAM to extract localization maps from CLIP was employed in a zero-shot setting. Specifically, we considered two variants of this method: CLIP-ES (GT-Known) and CLIP-ES (Pred). The CLIP-ES (GT-Known) variant requires ground-truth class labels during inference to generate localization maps. While this provides an upper bound on performance, it relies on privileged information unavailable in practical WSOL scenarios, thereby limiting its applicability. In contrast, CLIP-ES (Pred) depends solely on predicted class labels, aligning with the standard weakly supervised setting and offering a fair basis for comparison. This comprehensive evaluation enables us to demonstrate the robustness of our method across diverse settings.

## 4.2. Comparison with State-of-the-Art

**Quantitative results.** TeD-Loc sets a new benchmark in WSOL by achieving SOTA results across different measures. On the ILSVRC dataset, TeD-Loc attains a **MaxBoxAcc** of 75.6%, Top-1 localization accuracy of 70.0%, and Top-5 localization accuracy of 75.1%, a significant improvement over existing methods. For instance, GenPrompt [15], which leverages Stable Diffusion and EfficientNet-B7, achieves a **MaxBoxAcc** of 75.0%, Top-1 localization accuracy of 65.2%, and Top-5 localization accuracy of 73.4%. Similarly, on the CUB dataset, TeD-Loc excels by achieving a **MaxBoxAcc** of 98.7%, Top-1 localization accuracy of 91.7%, and Top-5 localization accuracy of 97.6%. This surpasses the previous best method, GenPrompt [15], which reports a **MaxBoxAcc** of 98.0%, Top-1 localization accuracy of 87.0%, and Top-5 localization accuracy of 96.1%. The substantial gains on both datasets underscore the effectiveness of TeD-Loc in handling diverse and challenging scenarios.

The first two rows of Tab.1 pertain to CLIP-ES method [1], which utilizes the CLIP model in a zero-shot setting. Notably, CLIP-ES (GT-Known) uses GT class labels to generate predictions. This approach yields a high **MaxBoxAcc** of 74.2% on ILSVRC and 92.8% on CUB, respectively. Moreover, TeD-Loc achieves a Top-1 CL accuracy of 89.9% on the ILSVRC dataset, significantly outperforming CLIP, which achieves 67.3%. Additionally, on the CUB dataset, TeD-Loc attains a Top-1 CL accuracy of 93.0%, compared to CLIP’s 46.42%. This highlights the significance of learning from text embeddings and using them as anchors to compute classification scores. Furthermore, extended results are presented in suppl. materials.

It is interesting to observe that if we simplify the task for CLIP by using only the general “bird” class for all categories in the CUB dataset, the performance can increase by 4% when measuring **MaxBoxAcc**. However, this does not reflect the model’s ability to handle fine-grained classification and localization, which is essential for applications requiring precise object differentiation.

**Qualitative results.** Fig.4 presents a visual comparison of our method against recent state-of-the-art WSOL approaches, specifically GenPrompt [15] and TS-CAM [13], on the ILSVRC dataset. While these methods yield competitive quantitative performance, they often struggle with accurately localizing complex objects. They tend to highlight irrelevant parts or even entirely different objects, especially in intricate scenes. GenPrompt, for instance, relies on CLIP’s discriminative and representative embeddings during inference, which necessitates class labels at test time using the external classifier. While this approach aims to adaptively focus on the object of interest, it can erroneously localize incorrect objects when the classifier predicts the wrong class. This dependency on class information during inference increases the chances of mistakes, especially in critical applications where precise localization without prior class knowledge is required. In contrast, our method consistently achieves high localization accuracy by effectively capturing both discriminative and non-discriminative regions of the target object. These localization maps can produce bboxes that encompass the entire object, enhancing both localization performance and interpretability. Unlike other methods that produce low-activation regions—resulting in bboxes over areas without meaningful content—our approach ensures that activations correspond closely with the actual visual appearance of the object.

**Ablations.** Tab.2 shows that the combination of our proposed loss functions: knowledge-distillation loss ( $\mathbf{L}_{KD}$ ), patch classifier loss ( $\mathbf{P}_{CL}$ ) and global image classification loss ( $\mathbf{I}_{CL}$ ), is essential for achieving state-of-the-art localization performance. Using only the main loss  $\mathbf{L}_{KD}$ , our method yields a **MaxBoxAcc** of 62.3%, **MaxBoxAcc** of 62.3%, as it focuses on learning FG embeddings without yielding explicit localization, thereby explaining its limited performance. Adding patch classifier loss significantly improves accuracy to 95.4% by enhancing FG/BG separation. Finally, incorporating image class loss boosts the performance to 98.7%, emphasizing the importance of discriminative learning to distinguish between correct and incorrect class alignments. This demonstrates the effect of integrating these losses to achieve highly accurate weakly supervised object localization.

Method	Backbone		ILSVRC			CUB		
	CL	Loc	MaxBoxAcc	Top-1 Loc	Top-5 Loc	MaxBoxAcc	Top-1 Loc	Top-5 Loc
CLIP-ES [1] ( <i>cvpr,2023</i> )	Text & Vision: ViT		74.2	43.0	62.9	92.8	36.3	67.2
TS-CAM [13] ( <i>iccv,2021</i> )	DeiT-S		67.7	53.4	64.3	71.3	83.8	87.7
SCM [38] ( <i>eccv,2022</i> )	DeiT-S		68.8	56.1	66.4	76.4	91.6	96.6
LCTR [39] ( <i>aaai,2022</i> )	DeiT-S		68.7	56.1	65.8	92.4	79.2	89.9
PSOL [19] ( <i>cvpr,2020</i> )	DenseNet161	EfficientNet-B7	66.3	58.0	65.0	91.8	80.9	90.0
C <sup>2</sup> AM [40] ( <i>cvpr,2022</i> )	DenseNet161	EfficientNet-B7	68.5	59.6	67.1	92.9	81.8	91.1
GenPrompt [15] ( <i>iccv,2023</i> )	Stable Diffusion	EfficientNet-B7	75.0	65.2	73.4	98.0	87.0	96.1
CATR [41] ( <i>iccv,2023</i> )	DeiT-S		69.2	56.9	66.6	94.9	79.6	92.0
DA-WSOL [42] ( <i>pami,2024</i> )	ResNet50		71.8	55.3	–	88.4	71.1	–
BAS [5] ( <i>ijcv,2024</i> )	InceptionV3		72.0	58.5	69.0	94.6	72.0	88.1
TeD-Loc (ours)	ViT-EVA-L		<b>75.6</b>	<b>70.0</b>	<b>75.1</b>	<b>98.7</b>	<b>91.7</b>	<b>97.6</b>

Table 1. Performance comparison of TeD-Loc with state-of-the-art methods on the ILSVRC and CUB datasets. The metrics reported are MaxBoxAcc, Top-1 Loc, and Top-5 Loc. The first two rows correspond to Grad-CAM for CLIP [1], where class labels are required to produce localization maps, making direct comparison unfair as it leverages privileged information. TeD-Loc outperforms existing methods without relying on ground-truth class labels or thresholds derived from ground-truth data.

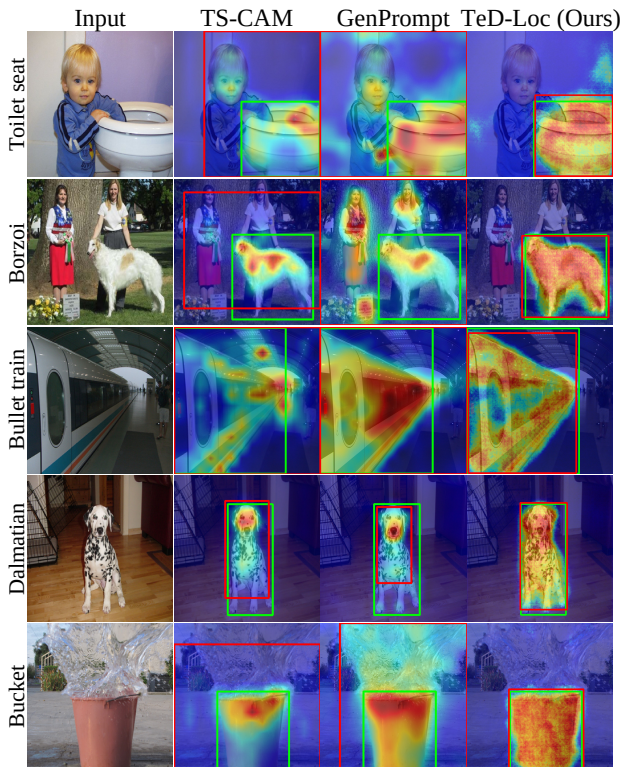


Figure 4. Qualitative comparison on the ILSVRC dataset. GenPrompt fails to localize objects in complex scenes, often due to its dependency on external classifiers for computing text embeddings, which can fail if the classifier makes mistakes. This dependence on class labels during inference highlights GenPrompt’s vulnerability to localization errors. In contrast, TeD-Loc can localize objects within complex scenes. Here, green bboxes denote GT localization, while red bboxes represent predicted localizations.

Losses	CUB (MaxBoxAcc)
$L_{KD}$	62.3
$L_{KD}+P_{CL}$	95.4
$L_{KD}+P_{CL}+I_{CL}$	<b>98.7</b>

Table 2. Ablation study on the CUB dataset showing the impact of different loss combinations on MaxBoxAcc performance.

### 4.3. Complexity Analysis

To show the efficacy of our proposed method, we presented a detailed complexity analysis (Tab.3) in comparison with two recent WSOL approaches: TS-CAM [13] and GenPrompt [15]. Although GenPrompt yields SOTA localization performance compared to TS-CAM, it introduces significant computational overhead. To deal with this issue, our method offers a computationally efficient model without sacrificing localization accuracy. TS-CAM utilizes a transformer-based architecture to generate class activation maps directly from image features. It maintains a relatively modest computational footprint, with 25.12 million parameters and an inference time of 19.04ms. Conversely, GenPrompt employs a generative framework involving diffusion models and CLIP embeddings to generate LOC maps, resulting in a considerable increase in complexity due to the multiple-modules pipeline and iterative nature of the diffusion process. Specifically, it comprises an EfficientNet-based classifier for label prediction (66.35 million parameters), a variational autoencoder (VAE) for latent embeddings (83.65 million parameters), and CLIP  $E_T$  for discriminative and representation embeddings, having 123.83 million parameters. The diffusion model, utilizing a U-Net



architecture, adds 859.5 million parameters and iterates across 100-time steps, drastically increasing computation time. Our proposed method thus emerges as a significantly more efficient alternative, achieving robust performance without the exorbitant computational cost characteristic of GenPrompt. Furthermore, for fair and consistent inference time measurement, we utilized an idle machine equipped with an NVIDIA-A100 GPU. We first conducted 20 warm-up epochs with a batch size of 1, followed by 1,000 inference steps, and calculated the average inference time across these steps.

Methods	Complexity Analysis		Top-1 Loc	
	# Para.	Infer. Time	ILSVRC	CUB
TS-CAM [13]	<b>25.12M</b>	<b>19.04ms</b>	53.4	83.8
GenPrompt [15]	1133.35M	272.90ms	65.2	87.0
TeD-Loc (ours)	569.67M	28.31ms	<b>70.0</b>	<b>91.7</b>

Table 3. Computational complexity and localization performance of our proposed TeD-Loc against GenPrompt and TS-CAM. For all method, we counted the number of parameters for modules that are being utilized just in inference.

## 5. Conclusion

We have introduced TeD-Loc, a novel approach that integrates textual and visual modalities by transferring knowledge directly from CLIP’s text embeddings to our patch embedding module. This alignment enables our model to localize objects at the patch-level while simultaneously performing classification. TeD-Loc exemplifies how the fusion of language and visual information can help in WSOL, demonstrating that classification can be achieved through localization, we discover that bridging modalities is not only feasible but also beneficial for complex vision tasks. Future research could explore deeper integrations of multimodal embeddings and extend this framework to other domains requiring weak supervision.

## 6. Supplementary material

This supplementary material contains the following content:

- A) Sampling FG/BG regions for pseudo-label generation.
- B) Extended results:
  - B.1) Patch-level Localization with text-anchors.
  - B.2) Impact of orthogonalization on results.
  - B.3) Extended complexity analysis.
- C) Code is provided in a zipped file.

## A. Sampling FG/BG Regions for Pseudo-label Generation

To train our model, we employ pseudo-labels for FG and BG regions following recent methods [3, 12, 32]. We obtain these pseudo-labels by utilizing CAM  $C \in \mathbb{R}^{H \times W}$  extracted from a pre-trained discriminative model, specifically using Grad-CAM [1] from CLIP [22]. These CAMs indicate regions of the image highlighting an object belonging to the FG class, and we use them to guide the sampling of FG and BG regions. We first apply Otsu’s thresholding method [43] to the CAM  $C$  to segment FG and BG regions. This method automatically determines a threshold, effectively separating high-activation regions (FG) from low-activation ones (BG). We denote the set of pixel locations in the image domain as  $\Omega$ .

For FG sampling, we focus on regions with high activation values in  $C$ . Specifically, we select the top  $n^+$  pixels with the highest activation values inside the image, forming the set of potential FG locations  $\omega_+ \subset \Omega$ . We then randomly sample a subset of these locations to be used as FG samples during training. For BG sampling, we consider regions with low activation values in  $C$ . We select the bottom  $n^-$  pixels with the lowest activation values, excluding any pixels that are within the FG regions. This forms the set of potential BG locations  $\omega_- \subset \Omega$ . We randomly sample from these locations to obtain BG samples for training. We note by  $\omega = \omega_+ \cup \omega_-$  the set of all sampled pixels in both FG and BG in one sampling step.

To ensure that our model generalizes well and avoids overfitting, we perform this sampling process at every training step for each image. This dynamic sampling allows the model to explore different regions of the image during training, promoting robustness and consistency in learning.

The sampled FG and BG pixel locations are used to create a partial pseudo-label mask  $y'_p \in \{0, 1\}$ , where  $y'_p = 1$  for FG pixels,  $y'_p = 0$  for BG pixels, and locations with unknown labels are left undefined. The set of sampled locations  $p$  is defined by  $p \in \omega$ .

## B. Extended Results

This section provides additional results to gain further insight into our method.

### B.1. Patch-level Localization with Text Anchors

In standard CLIP model [22], text class embedding is not necessarily correlated with the local vision patch embedding. To show this, we conduct the following experiment: consider the text embedding of the image class label  $y: t_y$ . Then, to localize this class object

within the image, we perform a dot product across all patch embeddings:  $\langle z_p, t_y \rangle$  where  $z_p, \forall p \in \Omega$ . High scores at location  $p$  should indicate the high likelihood of the object  $y$  presence at this location. The obtained score map is then considered as a CAM. We perform this experiment over three variants of CLIP model: Vanilla CLIP [22], SCLIP [24], and NACLIP [25], in addition to our method. The obtained results are presented in Tab.4. Vanilla CLIP yielded poor results confirming that class text embeddings are not necessarily correlated with the local patch embeddings making them less useful for this task. This justifies using a gradient-based method over the dot product score between the global image embedding and a class text embedding in CLIP-ES [1]. However, we notice a greater improvement in localization for the next recent CLIP variants SCLIP [24], and NACLIP [25]. However, their **Top-1**, and **Top-5 Loc** are still low indicating poor classification performance. On the other hand, our method achieves the highest performance over the three metrics indicating better localization and classification scores over both datasets. This is the result of our text-to-patch distillation, which ensures that local patch embeddings are correlated with the class text embedding, allowing direct localization based on the text embedding. This equips our method with a secondary localization approach and the patch FG/BG classifier  $g$ . This second localization approach yielded relatively better performance than when using  $g$ . Fig. 5 visualizes this localization strategy of different CLIP variants and our method.

Localization via $\langle z_p, t_y \rangle$	CUB			ILSVRC		
	MaxBoxAcc	Top-1 Loc	Top-5 Loc	MaxBoxAcc	Top-1 Loc	Top-5 Loc
Vanilla CLIP [22]	18.8	8.9	15.2	41.1	26.6	37.0
SCLIP (CoRR'23) [24]	85.8	14.4	37.1	70.4	33.9	55.1
NACLIP (wacv'25) [25]	80.8	12.0	32.3	71.7	28.6	49.4
TeD-Loc (ours)	<b>98.7</b>	<b>92.0</b>	<b>97.5</b>	<b>77.18</b>	<b>71.8</b>	<b>76.7</b>

Table 4. Localization performance via (patch, class) embeddings dot product:  $\langle z_p, t_y \rangle$  where  $z_p, \forall p \in \Omega$  is the patch embeddings, and  $y$  is the true image class. We report localization performance (**MaxBoxAcc**, **Top-1 Loc**, **Top-5 Loc**) using different variants of CLIP, and our method.

## B.2. Impact of Orthogonalization on Performance

Tab. 5 shows the impact of orthogonalization of class text embedding in our method for both tasks: classification and localization. These results suggest that original class text embeddings of CLIP [22] are not well adequate to perform discriminative learning as these embeddings overlap as shown visually in the main paper (Fig.3). However, their orthogonalization allows better separation of these embeddings making them more suitable for classification task. This also posi-

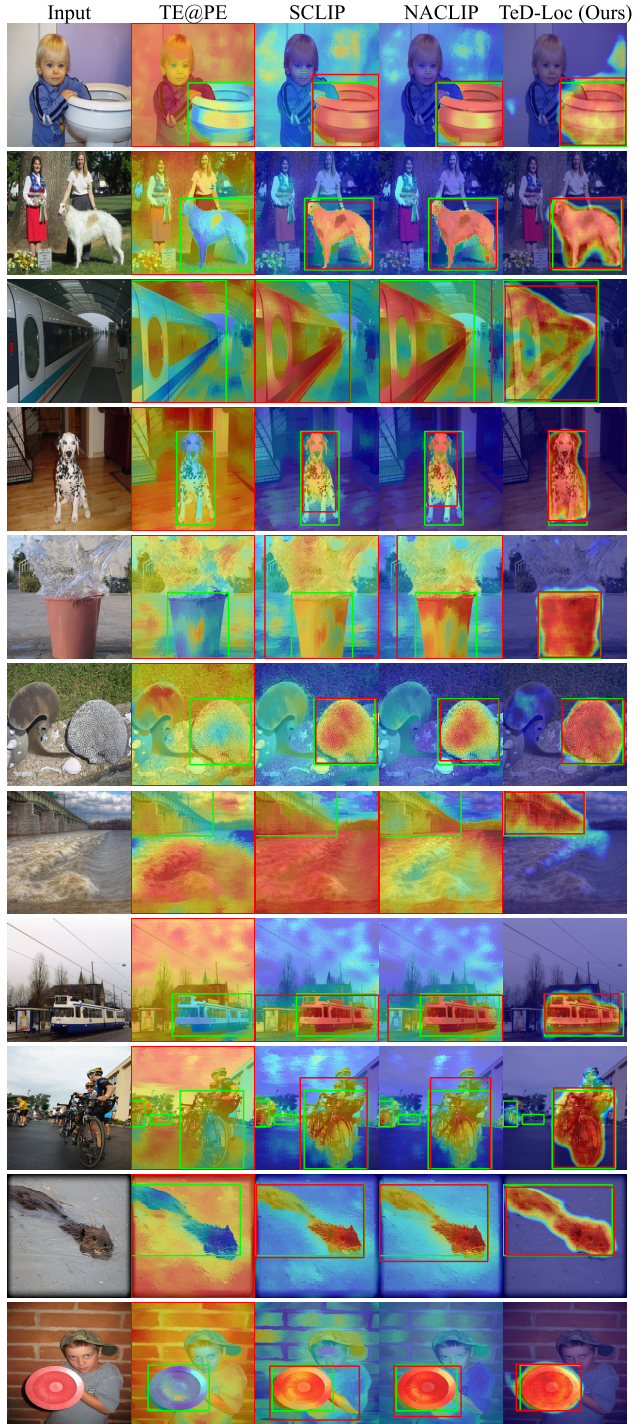


Figure 5. Visualization of localization map defined via (patch, class) embeddings dot product:  $\langle z_p, t_y \rangle$  where  $z_p, \forall p \in \Omega$  is the patch embeddings, and  $y$  is the true image class over different variants of CLIP, and our method. TE@PE is the vanilla CLIP [22] where TE is the text embedding, and PE is the patch embedding.

Method	MaxBoxAcc	CUB			
		CL	Top-1	Loc	Top-5
w/o orthogonalization (default anchors)	97.73	56.00	54.84		85.79
w/ orthogonalization	<b>98.7</b>	<b>93.0</b>	<b>91.7</b>		<b>97.6</b>

Table 5. Impact of class text embeddings (text anchors) orthogonalization over localization and classification performance in our method over **CUB** dataset.

tively affects localization as well in our method since both tasks are strongly related by design.

### B.3. Extended Complexity Analysis

Table 6 shows a comparison in terms of complexity between GenPrompt [15], TS-CAM [13] and our method. In terms of parameters, GenPrompt [15] hits more than 1B parameters, followed by our method with half of that, then, TS-CAM [13] with roughly 25M parameters. During inference, and due to the diffusion generation steps, GenPrompt can easily yield several TFLOPS, depending on the number of steps  $m$  making it the most expensive approach. This is directly reflected in the inference time. This shows that our method provides a relatively fast method with high localization and classification performance. All computations are done using an input image size of  $224 \times 224$  for our method and TS-CAM [13] while GenPrompt [15] requires  $512 \times 512$  images. We also used an Nvidia A1000 GPU.

Methods	Complexity Analysis			Top-1 Loc		
	# Para.	FLOPS	MACs	Infer. Time	ILSVRC	CUB
TS-CAM [13]	25.12M	9.85G	4.92G	19.04ms	53.4	83.8
GenPrompt [15]	1133.35M	5.16T	2.57T	272.90ms	65.2	87.0
TeD-Loc (ours)	569.67M	3.7T+741.5G×m	1.8T+370.1G×m	28.31ms	<b>70.0</b>	<b>91.7</b>

Table 6. Computational complexity and localization performance of our proposed TeD-Loc against GenPrompt [15] and TS-CAM [13]. For all methods, we counted the number of parameters for modules that are being utilized just in inference. Here  $m$  is the number of steps, and it varies from 2 to 99 steps.

## References

- [1] Y. Lin, M. Chen, W. Wang, B. Wu, K. Li, B. Lin, H. Liu, and X. He, “CLIP is also an efficient segmenter: A text-driven approach for weakly supervised semantic segmentation,” in *CVPR*, 2023. **1, 2, 3, 7, 8, 9, 10**
- [2] B. Zhou, A. Khosla, A. Lapedriza, A. Oliva, and A. Torralba, “Learning deep features for discriminative localization,” in *CVPR*, 2016. **1, 3**
- [3] S. Belharbi, A. Sarraf, M. Pedersoli, I. B. Ayed, L. McCaffrey, and E. Granger, “F-CAM: Full resolution class activation maps via guided parametric upscaling,” in *WACV*, 2022. **1, 2, 5, 9**
- [4] W. Lu, X. Jia, W. Xie, L. Shen, Y. Zhou, and J. Duan, “Geometry constrained weakly supervised object localization,” in *ECCV* (A. Vedaldi, H. Bischof, T. Brox, and J. Frahm, eds.), pp. 481–496, 2020. **2**
- [5] P. Wu, W. Zhai, and Y. Cao, “Background activation suppression for weakly supervised object localization,” in *CVPR*, pp. 14228–14237, IEEE, 2022. **3, 7, 8**
- [6] H. Xue, C. Liu, F. Wan, J. Jiao, X. Ji, and Q. Ye, “Danet: Divergent activation for weakly supervised object localization,” in *CVPR*, 2019.
- [7] S. Yun, D. Han, S. J. Oh, S. Chun, J. Choe, and Y. Yoo, “Cutmix: Regularization strategy to train strong classifiers with localizable features,” in *ICCV*, pp. 6023–6032, 2019. **3**
- [8] X. Zhang, Y. Wei, G. Kang, Y. Yang, and T. Huang, “Self-produced guidance for weakly-supervised object localization,” in *ECCV*, 2018. **2, 3**
- [9] X. Zhang, Y. Wei, J. Feng, Y. Yang, and T. Huang, “Adversarial complementary learning for weakly supervised object localization,” in *CVPR*, 2018. **2, 3**
- [10] J. Choe and H. Shim, “Attention-based dropout layer for weakly supervised object localization,” in *CVPR*, 2019. **3**
- [11] J. Choe, S. Lee, and H. Shim, “Attention-based dropout layer for weakly supervised single object localization and semantic segmentation,” *IEEE TPAMI*, pp. 4256–4271, 2021. **2**
- [12] S. Murtaza, S. Belharbi, M. Pedersoli, A. Sarraf, and E. Granger, “Discriminative sampling of proposals in self-supervised transformers for weakly supervised object localization,” in *WACVw*, pp. 155–165, 2023. **2, 9**
- [13] W. Gao, F. Wan, X. Pan, Z. Peng, Q. Tian, Z. Han, B. Zhou, and Q. Ye, “TS-CAM: Token semantic coupled attention map for weakly supervised object localization,” in *ICCV*, 2021. **2, 3, 7, 8, 9, 11**
- [14] J. Wang and G. Kang, “Learn to rectify the bias of clip for unsupervised semantic segmentation,” in *CVPR*, pp. 4102–4112, 2024. **2, 5**
- [15] Y. Zhao, Q. Ye, W. Wu, C. Shen, and F. Wan, “Generative prompt model for weakly supervised object localization,” in *CVPR*, pp. 6351–6361, 2023. **2, 7, 8, 9, 11**
- [16] W. GANDER, “Algorithms for the qr-decomposition,” 1980. **2, 5**
- [17] K. K. Singh and Y. J. Lee, “Hide-and-seek: Forcing a network to be meticulous for weakly-supervised object and action localization,” in *ICCV*, 2017. **3, 6**
- [18] X. Pan, Y. Gao, Z. Lin, F. Tang, W. Dong, H. Yuan, F. Huang, and C. Xu, “Unveiling the potential of structure preserving for weakly supervised object localization,” in *CVPR*, pp. 11642–11651, 2021. **3**
- [19] C.-L. Zhang, Y.-H. Cao, and J. Wu, “Rethinking the route towards weakly supervised object localization,” in *CVPR*, 2020. **3, 7, 8**
- [20] G. Sharir, A. Noy, and L. Zelnik-Manor, “An image is worth 16x16 words, what is a video worth?,” *arXiv preprint arXiv:2103.13915*, 2021. **3**

- [21] N. Carion, F. Massa, G. Synnaeve, N. Usunier, A. Kirillov, and S. Zagoruyko, “End-to-end object detection with transformers,” in *ECCV*, Springer, 2020. [3](#)
- [22] A. Radford, J. Kim, C. Hallacy, and et al, “Learning transferable visual models from natural language supervision,” in *ICML*, 2021. [3](#), [5](#), [9](#), [10](#)
- [23] J. Xie, X. Hou, K. Ye, and L. Shen, “CLIMS: Cross language image matching for weakly supervised semantic segmentation,” in *CVPR*, 2022. [3](#)
- [24] F. Wang, J. Mei, and A. Yuille, “Sclip: Rethinking self-attention for dense vision-language inference,” *arXiv preprint arXiv:2312.01597*, 2023. [3](#), [10](#)
- [25] S. Hajimiri, I. B. Ayed, and J. Dolz, “Pay attention to your neighbours: Training-free open-vocabulary semantic segmentation,” *arXiv preprint arXiv:2404.08181*, 2024. [4](#), [10](#)
- [26] X. Yang and X. Gong, “Foundation model assisted weakly supervised semantic segmentation,” in *WACV*, 2024. [4](#)
- [27] A. Kirillov, E. Mintun, N. Ravi, H. Mao, C. Rolland, L. Gustafson, T. Xiao, S. Whitehead, A. C. Berg, W.-Y. Lo, *et al.*, “Segment anything,” in *ICCV*, 2023. [4](#)
- [28] Y. Fang, W. Wang, B. Xie, Q. Sun, L. Wu, X. Wang, T. Huang, X. Wang, and Y. Cao, “Eva: Exploring the limits of masked visual representation learning at scale,” in *CVPR*, pp. 19358–19369, 2023. [4](#)
- [29] J. Choe, S. Oh, S. Lee, S. Chun, Z. Akata, and H. Shim, “Evaluating weakly supervised object localization methods right,” in *CVPR*, 2020. [5](#), [6](#)
- [30] S. Murtaza, S. Belharbi, M. Pedersoli, and E. Granger, “A realistic protocol for evaluation of weakly supervised object localization,” in *IEEE WACV*, 2025.
- [31] J. Rony, S. Belharbi, J. Dolz, I. Ben Ayed, L. McCafrey, and E. Granger, “Deep weakly-supervised learning methods for classification and localization in histology images: A survey,” *Machine Learning for Biomedical Imaging*, vol. 2, pp. 96–150, 2023. [5](#)
- [32] S. Murtaza, S. Belharbi, M. Pedersoli, A. Sarraf, and E. Granger, “Dips: Discriminative pseudo-label sampling with self-supervised transformers for weakly supervised object localization,” *IVC Journal*, vol. 140, p. 104838, 2023. [5](#), [7](#), [9](#)
- [33] J. Deng, W. Dong, R. Socher, L. Li, K. Li, and L. Fei-Fei, “Imagenet: A large-scale hierarchical image database,” in *CVPR*, 2009. [5](#), [6](#)
- [34] S. Hajimiri, I. B. Ayed, and J. Dolz, “Pay attention to your neighbours: Training-free open-vocabulary semantic segmentation,” in *WACV*, 2025. [5](#)
- [35] C. Wah, S. Branson, W. Steve, P. Peter, and S. Belongie, “The caltech-ucsd birds-200-2011 dataset,” Tech. Rep. CNS-TR-2011-001, California Institute of Technology, 2011. [6](#)
- [36] B. Recht, R. Roelofs, L. Schmidt, and V. Shankar, “Do imagenet classifiers generalize to imagenet?,” in *ICML*, 2019. [6](#)
- [37] T. Deselaers, B. Alexe, and V. Ferrari, “Weakly supervised localization and learning with generic knowledge,” *IJCV*, vol. 100, pp. 275–293, 2012. [6](#)
- [38] H. Bai, R. Zhang, J. Wang, and X. Wan, “Weakly supervised object localization via transformer with implicit spatial calibration,” *ECCV*, 2022. [7](#), [8](#)
- [39] Z. Chen, C. Wang, Y. Wang, G. Jiang, Y. Shen, Y. Tai, C. Wang, W. Zhang, and L. Cao, “LCTR: on awakening the local continuity of transformer for weakly supervised object localization,” in *AAAI*, pp. 410–418, 2022. [7](#), [8](#)
- [40] J. Xie, J. Xiang, J. Chen, X. Hou, X. Zhao, and L. Shen, “C2am: Contrastive learning of class-agnostic activation map for weakly supervised object localization and semantic segmentation,” in *CVPR*, pp. 989–998, 2022. [7](#), [8](#)
- [41] Z. Chen, J. Ding, L. Cao, Y. Shen, S. Zhang, G. Jiang, and R. Ji, “Category-aware allocation transformer for weakly supervised object localization,” in *ICCV*, pp. 6643–6652, 2023. [7](#), [8](#)
- [42] L. Zhu, Q. She, Q. Chen, Q. Ren, and Y. Lu, “Boosting weakly supervised object localization and segmentation with domain adaption,” *IEEE TPAMI*, 2024. [7](#), [8](#)
- [43] N. Otsu *et al.*, “A threshold selection method from gray-level histograms,” *Automatica*, vol. 11, no. 285–296, pp. 23–27, 1975. [9](#)